

Discrete-Time Passivity-Based Control using Hermite-Obreschkoff Methods ^{*,**}

Le Zhang^{*}, Paul Kotyczka^{*}

^{*} *Technical University of Munich, TUM School of Engineering and Design, Chair of Automatic Control, Garching, Germany (e-mail: le.zhang@tum.de, kotyczka@tum.de).*

Abstract: The motivation for this paper is the implementation of nonlinear state feedback control, designed based on the continuous-time plant model, in a sampled control loop under relatively slow sampling. In previous work we have shown that using one-step predictions of the target dynamics with higher order integration schemes, together with possibly higher order input shaping, is a simple and effective way to increase the feasible sampling times until performance degradation and instability occur. In this contribution we present a unifying derivation for arbitrary orders of the previously used Lobatto IIIA collocation and Hermite interpolation schemes through the Hermite-Obreschkoff formula. We derive, moreover, an IDA-PBC controller for a magnetic levitation system, which requires a non-constant target interconnection matrix, and show experimental results.

Keywords: Discrete-time control; Numerical integration; Nonlinear systems; Passivity-based control; Lobatto Collocation; Hermite Interpolation.

1. INTRODUCTION

Nonlinear, including passivity-based controls are typically derived in continuous time. In practice, the derived control laws are implemented on digital controllers (computers, programmable logic or micro-controllers), which operate in discrete time with sampled data. Frequently, the continuous control law is implemented directly on the digital controller, in a piecewise constant manner (zero order hold), which corresponds to using the discrete-time model issued from a first order explicit Euler discretization. With sufficiently high sampling frequencies, this simple implementation provides very satisfactory performance. However, for systems with fast dynamics, high sampling frequencies require high-end sensors that can be not only expensive, but also energy consuming. For some cases, it might even be impossible to sample and process the required signals at a sufficiently high rate. In these situations, the controllers suffer from significant performance degradation due to increasing model mismatch, which can lead to destabilization.

To reduce the model mismatch, while also ensuring that the control law designed in continuous time can be directly reused, we initially proposed a second-order discrete-time implementation using the implicit midpoint rule (Kotyczka and Thoma, 2021). Later, we extended the approach to s -stage Gauss-Legendre collocation with higher order input shaping (Kotyczka et al., 2021). In Kotyczka (2023), we discussed the sampled control implementation with cubic Hermite interpolation or 3-stage Lobatto IIIA collocation,

which are equivalent symmetric methods, and can potentially reduce the discontinuity of the control signal at the sampling instants.

The topic of this contribution is to generalize the two methods implemented in Kotyczka (2023) towards Hermite-Obreschkoff (HO) methods. We show that Lobatto IIIA collocation of *arbitrary* order can be derived using the HO formula, and that the derivation gives rise to a specific set of interpolation splines of the corresponding order. We argue that this interpolation scheme is equivalent to Hermite interpolation after some mathematical manipulation. We further present the use of this interpolation scheme in practical implementation on a magnetic levitation experiment, where the passivity-based control design with the IDA-PBC method (Ortega et al., 2002) requires a non-constant interconnection matrix due to the form of the distance-dependent inductance function.

In Section 2, we first introduce the HO formula under the setting of solving an initial value problem (IVP). We then show respectively the derivation of Lobatto IIIA collocation and the corresponding interpolation schemes using this formula. In Section 3, we recall the higher-order input shaping introduced in previous works. As a workaround to prevent strongly oscillating inputs due to their polynomial shape and modeling inaccuracies, we propose how to convert the control to a piecewise constant (zero order hold) signal. In Section 4, we present the novel IDA-PBC controller for the magnetic levitation system and discuss some experimental observations regarding its discrete-time implementation.

^{*} Submitted to the 13th IFAC Symposium on Nonlinear Control Systems 2025.

^{**}Funded by the Deutsche Forschungsgemeinschaft (DFG, German Research Foundation) – 543741503.

2. SOLVING INITIAL VALUE PROBLEMS USING HERMITE-OBRESCHKOFF METHODS

We consider a time-varying initial value problem of the form

$$\dot{x}(t) = f(t, x(t)), \quad x(t_k) = x_k, \quad (1)$$

on an arbitrary time interval $I_k = [t_k, t_{k+1}]$, $t_k = kh$, $h = \text{const.}$, $k \in \mathbb{N}_0$ (equidistant sampling).

2.1 Hermite-Obreschkoff Formula

Obreschkoff (1940) suggested the following new quadrature formula based on Taylor series and Cesàro summation (Cesàro, 1890):

$$\sum_{j=0}^n A_n^{m-j} \frac{(\tau h)^j}{j!} \frac{d^j}{dt^j} x(t_k) = \sum_{j=0}^m A_n^{m-j} \frac{(-\tau h)^j}{j!} \frac{d^j}{dt^j} \tilde{x}(t_k + \tau h), \quad (2)$$

where $x(t)$ is assumed to be $(n+m+1)$ -times differentiable, $n, m \in \mathbb{N}_0$, $\tau \in [0, 1]$, and

$$A_n^m = \binom{n+m}{n} = \frac{(n+m)!}{n!m!}. \quad (3)$$

The “ \sim ” sign on the right-hand-side of (2) indicates that $\tilde{x}(t_k + \tau h)$ is an approximation, which has a local error of $\mathcal{O}(h^{n+m+1})$ (Obreschkoff, 1940).

The general idea of HO methods is to combine the HO formulas defined by different choices of the integer pair (n, m) , while the local errors remain the same order, i.e., $n + m$ stays constant. This consistency allows the local error of the resulting method to have the same order, and avoids confusion in the truncation error. We call the resulting numerical integration scheme from such a combination an Hermite-Obreschkoff method.

2.2 Lobatto IIIA Collocation

We now show that the Lobatto IIIA collocation schemes are members of the HO methods, in the sense that they can be derived through the combination of HO formulas.

The collocation points used in Lobatto IIIA methods are the zeros of the shifted Legendre polynomial

$$\frac{d^{s-2}}{dx^{s-2}} (x^{s-1} (x-1)^{s-1}), \quad (4)$$

where the integer $s \geq 2$ is the number of collocation points (the number is no smaller than 2 since there are at least 0 and 1), see Hairer et al. (2006). We denote these points as c_i , $i = 1, \dots, s$ (where $c_1 = 0$, $c_s = 1$). By substituting τ in (2) with each c_i , the Lobatto IIIA collocation schemes can be derived.

Theorem 1. If the nodes c_i , $i = 1, \dots, s$, in which the integer $s \geq 2$, are the zeros of (4), then the Hermite-Obreschkoff method using the pairs $(s, 0)$ and $(s-1, 1)$ is equivalent to the s -stage Lobatto IIIA method.

Proof. For convenience, we first introduce some notation. For the state variable, we denote

$$x_k := x(t_k), \quad \tilde{x}_{k,i} := \tilde{x}(t_k + c_i h).$$

For the time derivatives, we use the flow symbol f :

$$\begin{aligned} \tilde{f}_{k,i}^{(j-1)} &:= \frac{d^{j-1}}{dt^{j-1}} f(t_k + c_i h, \tilde{x}(t_k + c_i h)) = \frac{d^j}{dt^j} \tilde{x}(t_k + c_i h), \\ \tilde{f}_k^{(j-1)} &:= \frac{d^{j-1}}{dt^{j-1}} f(t_k, x(t_k)) = \frac{d^j}{dt^j} x(t_k), \quad i, j = 1, \dots, s. \end{aligned}$$

For now we do not wish to involve time derivatives of the flow at the nodes, i.e., m cannot be greater than 1. Choosing the integer pair (n, m) to be $(s, 0)$ and $(s-1, 1)$ respectively, (2) yields two “master” equations

$$\tilde{x}_{k,i} = x_k + \sum_{j=1}^s \frac{(c_i h)^j}{j!} \tilde{f}_k^{(j-1)}, \quad (5)$$

$$s\tilde{x}_{k,i} - c_i h \tilde{f}_{k,i} = s x_k + \sum_{j=1}^{s-1} (s-j) \frac{(c_i h)^j}{j!} \tilde{f}_k^{(j-1)}. \quad (6)$$

With the nodes c_i , $i = 1, \dots, s$, (5) and (6) gives $2s$ equations in total. But we notice that for $c_1 = 0$, both (5) and (6) give the same equation $\tilde{x}_{k,1} = x_k$, which indicates $\tilde{f}_{k,1} = f_k$. Therefore, we have in fact $2s - 1$ equations, which can be written in the compact form

$$\begin{aligned} \begin{bmatrix} I_{s \times s} & P_{s \times (s-1)} \\ O_{(s-1) \times s} & Q_{(s-1) \times (s-1)} \end{bmatrix} \begin{bmatrix} \tilde{X} \\ \Delta_k \end{bmatrix} \\ = \begin{bmatrix} I_{s \times s} & M_{s \times s} \\ O_{(s-1) \times s} & N_{(s-1) \times s} \end{bmatrix} \begin{bmatrix} X_k \\ h\tilde{F} \end{bmatrix}, \end{aligned} \quad (7)$$

where \tilde{X} , Δ_k , X_k , \tilde{F} are matrices containing the variables

$$\begin{aligned} \tilde{X} &:= [\tilde{x}_{k,1}, \dots, \tilde{x}_{k,s}]^T, \quad \Delta_k := [f_k, \dots, f_k]^{(s-1)T}, \\ X_k &:= [x_k, \dots, x_k]^T, \quad \tilde{F} := [f_{k,1}, f_{k,2}, \dots, f_{k,s}]^T, \end{aligned} \quad (8)$$

and P, Q, M, N are constant matrices, whose dimensions are indicated by their subscripts.

According to (5) and (6), the elements of the matrices P, Q are verified to be

$$P_{i,j} = -\frac{(c_i h)^{j+1}}{(j+1)!}, \quad i = 1, \dots, s, \quad j = 1, \dots, s-1, \quad (9)$$

$$Q_{i,j} = -\frac{1}{s} \frac{(c_{i+1} h)^{j+1}}{j!}, \quad i, j = 1, \dots, s-1. \quad (10)$$

And M, N turn out to be

$$M = \begin{bmatrix} c_1 & 0 & \dots & 0 \\ \vdots & \vdots & & \vdots \\ c_s & 0 & \dots & 0 \end{bmatrix}, \quad N = \frac{1}{s} \begin{bmatrix} c_2 & -c_2 & 0 & \dots & 0 \\ c_3 & 0 & -c_3 & \dots & 0 \\ \vdots & \vdots & \vdots & \ddots & \vdots \\ c_s & 0 & 0 & \dots & -c_s \end{bmatrix}. \quad (11)$$

Now that (7) is well defined, we can make the observation that if the nodes c_2, \dots, c_s are distinct from each other (which is true by their definition), and the sampling time h is non-zero, then Q is invertible, and (7) yields the unique solution

$$\tilde{X} = X_k + h A_s \tilde{F}, \quad (12)$$

in which the coefficient matrix A_s is defined as

$$A_s := M - P Q^{-1} N. \quad (13)$$

For a given integer s , (12) gives the exactly same formulation as the s -stage Lobatto IIIA collocation shown in Hairer et al. (2006).

Remark 2. We have defined the matrices as in (8) to avoid the Kronecker product. In terms of the stacked column vectors of $\text{vec}(\tilde{X}^T)$, (12) would read

$$\text{vec}(\tilde{X}^T) = \text{vec}(X_k^T) + h(A_s \otimes I) \text{vec}(\tilde{F}^T). \quad (14)$$

Remark 3. By setting the pair (n, m) to be $(s, 0)$ and $(s - 1, 1)$, we ensure that the resulting HO method is an approximation of order s . However, the corresponding s -stage Lobatto IIIA collocation is an approximation of order $2s - 2$ (Hairer et al., 2006). Therefore, the HO method only provides a very conservative evaluation on the approximation order. For an accurate evaluation of the approximation order, we refer to the “rooted-tree-type” theory presented in Jay (1994), and the proof of *superconvergence* presented in Hairer et al. (2006).

Example. For $s = 2$ and $s = 3$, the nodes are $\{0, 1\}$ and $\{0, \frac{1}{2}, 1\}$ respectively. Using (13), the coefficient matrices are

$$A_2 = \begin{bmatrix} 0 & 0 \\ \frac{1}{2} & \frac{1}{2} \end{bmatrix}, \quad A_3 = \begin{bmatrix} 0 & 0 & 0 \\ \frac{5}{24} & \frac{1}{3} & -\frac{1}{24} \\ \frac{1}{6} & \frac{2}{3} & \frac{1}{6} \end{bmatrix}, \quad (15)$$

which are indeed identical to those of the 2- and 3-stage Lobatto IIIA collocation written as Runge–Kutta schemes.

2.3 Hermite Interpolation

The derivation of Lobatto IIIA collocation only makes use of HO formulas with the pairs $(s, 0)$ and $(s - 1, 1)$. Now we investigate other pairs with the same order.

Firstly, we assume the pair is now $(s - m, m)$, $m = 2$. This pair exists since $s \geq 2$. A new “master” equation for this pair is

$$\begin{aligned} & A_{s-m}^m s \tilde{x}_{k,i} - A_{s-m}^{m-1} c_i h \tilde{f}_{k,i} + \sum_{j=2}^m A_{s-m}^{m-j} \frac{(-c_i h)^j}{j!} \tilde{f}_{k,i}^{(j-1)} \\ &= A_{s-m}^m x_k + \sum_{j=1}^{s-m} A_{s-m-j}^m \frac{(c_i h)^j}{j!} f_k^{(j-1)}, \end{aligned} \quad (16)$$

which yields $s - 1$ new equations with c_i , $i = 2, \dots, s$ (with $c_1 = 0$ we get $\tilde{x}_{k,1} = x_k$ again). Comparing (16) with (6), the main difference is the new unknown variables

$$\tilde{f}_{k,2}^{(m-1)}, \dots, \tilde{f}_{k,s}^{(m-1)}.$$

Since all the other variables are determined by (7), we can express these new unknowns as functions of \tilde{F} , and move them all to the right-hand-side. (16) thus becomes

$$\frac{(-h)^m}{m!} \begin{bmatrix} c_2^m & & \\ & \ddots & \\ & & c_s^m \end{bmatrix} \begin{bmatrix} (\tilde{f}_{k,2}^{(m-1)})^T \\ \vdots \\ (\tilde{f}_{k,s}^{(m-1)})^T \end{bmatrix} = E_{(s-1) \times s} \tilde{F}, \quad (17)$$

where E represent some constant matrix dependent on h and c_i . Since h is non-zero, and the nodes are distinct from each other, these $s - 1$ new unknowns can also be uniquely solved for. Should s be greater than 2, the exactly same process can be carried out for each $m = 3, \dots, s$.

As the second step, we define the following matrices

$$\dot{\tilde{F}} = [\dot{f}_{k,1}, \dots, \dot{f}_{k,s}]^T, \quad \dots, \quad \tilde{F}^{(s-1)} = [f_{k,1}^{(s-1)}, \dots, f_{k,s}^{(s-1)}]^T, \quad (18)$$

in which $\tilde{f}_{k,1}^{(j)} = f_k^{(j)}$, $j = 1, \dots, s - 1$, is determined by (7), and the rest can be solved for with (17). Together with \tilde{X} , we have s^2 variables to be solved for.

On the other hand, using all the pairs (n, m) satisfying $n + m = s$, and the s nodes, the HO formula yields s^2 equations in total (removing the identical equations). Through the process above (including Section 2.2), we show that these s^2 equations are actually *linearly independent* with respect to the s^2 variables. Therefore, they can be solved uniquely and also efficiently.

We can organize all the solutions in a uniform manner:

$$\begin{aligned} \tilde{F}^{(s-1)} &= \frac{1}{h^{s-1}} D_s^{(s-1)} \tilde{F}, \\ &\vdots \\ \dot{\tilde{F}} &= \frac{1}{h} D_s^{(1)} \tilde{F}, \\ \tilde{F} &= D_s^{(0)} \tilde{F}, \\ \tilde{X} &= X_k + h A_s \tilde{F}, \end{aligned} \quad (19)$$

where A_s is defined by (13), $D_s^{(i)}$, $i = 0, \dots, s - 1$ are some constant coefficient matrices, among which $D_s^{(0)}$ is always the identity matrix, and the rest are computed through (7) and (17). Note that the second last equation is trivial, but deliberately added for the sake of uniformity, as \tilde{F} is not unknown. From another point of view, this equation actually represents the collocation condition.

Two observations can be made after (19) is computed:

- (1) All rows of $D_s^{(s-1)}$ are identical, suggesting that $\frac{d^{s-1}}{dt^{s-1}} f$ is approximated by a constant value across the time interval I_k .
- (2) Each equation is the time integral of the equation above it.

For the final step, we introduce the following notation to represent the approximations across the time interval I_k

$$\begin{aligned} \tilde{x}_{k+\tau} &:= \tilde{x}(t_k + \tau h), \\ \tilde{f}_{k+\tau}^{(j-1)} &:= \frac{d^{j-1}}{dt^{j-1}} f(t_k + \tau h, \tilde{x}(t_k + \tau h)), \quad j = 1, \dots, s, \end{aligned}$$

where $\tau \in [0, 1]$ is the normalized time. Note that $dt = h d\tau$, and therefore $\frac{d}{dt} = \frac{1}{h} \frac{d}{d\tau}$.

Now we express all the approximations involved in (19) using τ :

$$\begin{aligned} \tilde{f}_{k+\tau}^{(s-1)} &= \frac{1}{h^{s-1}} \tilde{F}^T \frac{d^s}{d\tau^s} H_s(\tau), \\ &\vdots \\ \dot{\tilde{f}}_{k+\tau} &= \frac{1}{h} \tilde{F}^T \frac{d^2}{d\tau^2} H_s(\tau), \\ \tilde{f}_{k+\tau} &= \tilde{F}^T \frac{d}{d\tau} H_s(\tau), \\ \tilde{x}_{k+\tau} &= x_k + h \tilde{F}^T H_s(\tau), \end{aligned} \quad (20)$$

where $H_s(\tau)$ is a vector function of dimension s , of which each element is a polynomial of τ .

Based on the observations above, we can state that $(d^s/d\tau^s) H_s(\tau)$ is a constant vector, and each element of $H_s(\tau)$ is a polynomial of order s , meaning that it contains

$s(s+1)$ coefficients to be defined. By matching (20) at the nodes with (19), we get

$$\begin{bmatrix} \frac{d^i}{d\tau^i} H_s(c_1) & \cdots & \frac{d^i}{d\tau^i} H_s(c_s) \\ H_s(c_1) & \cdots & H_s(c_s) \end{bmatrix} = (D_s^{(i-1)})^T, \quad i = 1, \dots, s, \\ [H_s(c_1) \quad \cdots \quad H_s(c_s)] = A_s^T. \quad (21)$$

By solving (21), $H_s(\tau)$ is well defined, and we derive an interpolation scheme, which we formulate below.

Definition 4. If the nodes c_i , $i = 1, \dots, s$, in which the integer $s \geq 2$, are the zeros of (4), then the Hermite-Obreschkoff method using the pairs (n, m) satisfying

$$n + m = s, \quad n, m \in \mathbb{N}_0,$$

is an s -order Hermite interpolation scheme of the form

$$\tilde{x}(t_k + \tau h) = x_k + h\tilde{F}^T H_s(\tau), \quad \tau \in [0, 1], \quad (22)$$

where $H_s(\tau)$ is a set of interpolation splines of order s .

Remark 5. The system of equations derived from (21) is actually overdetermined, as there are $s^2(s+1)$ equations, but only s^2 coefficients to be solved. Despite this, the system of equations is consistent and can be solved, indicating that some of them are actually linear combinations of others.

Example. For $s = 3$, it is computed that

$$D_3^{(2)} = \begin{bmatrix} 4 & -8 & 4 \\ 4 & -8 & 4 \\ 4 & -8 & 4 \end{bmatrix}, \quad D_3^{(1)} = \begin{bmatrix} -3 & 4 & -1 \\ -1 & 0 & 1 \\ 1 & -4 & 3 \end{bmatrix}, \quad (23)$$

and $D_3^{(0)} = I_3$, A_3 is defined in (15). The splines turn out to be

$$H_3(\tau) = \begin{bmatrix} \frac{2}{3}\tau^3 - \frac{3}{2}\tau^2 + \tau \\ -\frac{4}{3}\tau^3 + 2\tau^2 \\ \frac{2}{3}\tau^3 - \frac{1}{2}\tau^2 \end{bmatrix}, \quad \tau \in [0, 1]. \quad (24)$$

From the last row of (12), we have

$$\tilde{f}_{k,2} = -\frac{3}{2h}x_k + \frac{3}{2h}\tilde{x}_{k,3} - \frac{1}{4}\tilde{f}_{k,1} - \frac{1}{4}\tilde{f}_{k,3}. \quad (25)$$

Substituting (25) into (22), and replacing $\tilde{x}_{k,3}, \tilde{f}_{k,3}$ with $\tilde{x}_{k+1}, \tilde{f}_{k+1}$ (since $c_3 = 1$), (22) becomes

$$\tilde{x}(t_k + \tau h) = [x_k \quad \tilde{x}_{k+1}] \begin{bmatrix} 2\tau^3 - 3\tau^2 + 1 \\ -2\tau^3 + 3\tau^2 \end{bmatrix} + h [f_k \quad \tilde{f}_{k+1}] \begin{bmatrix} \tau^3 - 2\tau^2 + \tau \\ \tau^3 - \tau^2 \end{bmatrix}, \quad (26)$$

which is the cubic Hermite interpolation. Similarly, the quintic Hermite interpolation can be derived.

In Kotyczka (2023), it was proven that numerical integration based on the cubic Hermite interpolation is equivalent to the 3-stage Lobatto IIIA collocation. In this contribution, we set out from a different start point, and find out that both of these methods are members of the HO methods, and they both actually stem from solving the same set of HO formulas defined by the same nodes (zeros of (4)).

Theorem 6. Numerical integration (solution of IVP (1)) based on the s -stage Lobatto IIIA collocation is equivalent to the Hermite interpolation of order s .

Proof. The proof process is shown above.

3. HIGHER-ORDER DISCRETE-TIME CONTROL IMPLEMENTATION

For the implementation in a sampled control loop of the HO methods introduced above, we first recall briefly the input shaping method as described in Kotyczka (2023), and then propose a new technique to generate piecewise constant input signals by utilizing the Hermite interpolation schemes.

3.1 Input Shaping Based on Lagrange Interpolation

For a given control system

$$\dot{x}(t) = f(t, x(t)) + g(t, x(t))u(t), \quad x(0) = x_0, \quad (27)$$

and a state feedback law designed in continuous time

$$u(t) = r(t, x(t)), \quad (28)$$

the desired (subscript ‘‘d’’) closed-loop system is

$$\dot{x}(t) = f(t, x(t)) + g(t, x(t))r(t, x(t)) = f_d(t, x(t)). \quad (29)$$

Compute the parameters of the sampled control input as

$$u_{k,i} = r(t_k + c_i h, \tilde{x}_{k,i}), \quad i = 1, \dots, s, \quad (30)$$

then the control input signal on the sampling interval I_k is shaped using an $(s-1)$ -order-hold element according to

$$u(t_k + \tau h) = \sum_{i=1}^s \ell_i^{(s-1)}(\tau) u_{k,i}, \quad (31)$$

where $\ell_i^{(s-1)}(\tau)$ are Lagrange interpolation polynomials of degree $s-1$, defined as

$$\ell_i^{(s-1)}(\tau) = \prod_{j=1, j \neq i}^s \frac{\tau - c_j}{c_i - c_j}, \quad i = 1, \dots, s. \quad (32)$$

It was proven that, for sufficiently small h , if $\tilde{x}_{k,i}$ are the stage values of an order p accurate numerical solution of (29) on the sampling interval I_k (a one-step prediction of the target dynamics), then the trajectories of (27) with the shaped input (31) are approximations of order p of the desired closed-loop dynamics, see Kotyczka (2023).

3.2 Conversion to Piecewise Constant Input

The input shaping method using an $(s-1)$ -order hold element is theoretically sound, and provides very good performance. However, it requires the input signal to follow a high-order polynomial within one sampling interval, meaning that the actuators are operating at a much higher rate than the sensors. In practice and in other control implementations (such as model predictive control), this is often not the case. Should the actuators have the same operating rate as the sampling rate, then it is desired that the control signals are constant over one sampling interval.

Furthermore, when the sampling time is relatively long, or modeling errors and measurement noise are present, the shaped input tends to change in a large amplitude within one interval (as will be shown in the experimental results), which poses more challenges to the actuators.

We propose a *pragmatic* approach to calculate the average state evolution across the interval I_k :

$$\begin{aligned} \bar{x}_k &= \frac{1}{h} \int_{t_k}^{t_k+h} \tilde{x}(t) dt = \int_0^1 \tilde{x}(t_k + \tau h) d\tau \\ &= x_k + h\tilde{F}^T \int_0^1 H_s(\tau) d\tau, \end{aligned} \quad (33)$$

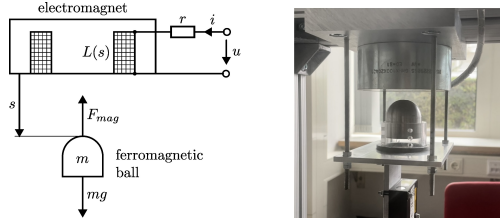


Fig. 1. Sketch and photo of the MagLev test bench.

and compute the control input as

$$u(t_k + \tau h) = r(\bar{x}_k). \quad (34)$$

We call this approach *pragmatic* for now, as it addresses the problem of practical implementation, but affects the convergent result of the embedded HO method. Additionally, this approach is only applicable when the control law $r(\cdot)$ is time-invariant.

4. EXPERIMENTAL RESULTS AND DISCUSSION

Finally, as validation, we implement Lobatto IIIA collocation and Hermite interpolation on the magnetic levitation system (MagLev) test bench, using both the higher-order shaped input and the piecewise constant input. First, we show the continuous-time control design of the MagLev using IDA-PBC, then we present the experimental results of its discrete-time implementation using the above mentioned HO methods.

4.1 IDA-PBC for the Magnetic Levitation System

The MagLev system is depicted in Fig. 1. Its continuous time dynamics can be described using the following:

$$\begin{aligned} \dot{s} &= \frac{p}{m}, \\ \dot{p} &= \frac{1}{2}L'(s)i^2 + mg, \\ \dot{i} &= -\frac{1}{L(s)}(r + L'(s)\frac{p}{m})i + \frac{1}{L(s)}u. \end{aligned} \quad (35)$$

The states s, p, i are the distance between the ball and the magnet, the momentum of the ball, and the electric current (always positive), the control input u is the voltage applied to the coil, and $L(s)$ is the inductance of the electromagnet identified as

$$L(s) = L_\infty + \frac{a}{(bs + 1)^3}, \quad L'(s) = -\frac{3ab}{(bs + 1)^4}. \quad (36)$$

This more precise inductance characteristic differs from the one used in Kotyczka et al. (2021), and requires a non-constant interconnection matrix for the IDA-PBC design. The identified system parameters are presented in Table 1.

The system has a strict-feedback form (Khalil, 2002), meaning that a fictitious control law $i^2 = \phi(s, p)$ can be

Table 1. System parameters

Name	Symbol	Value	Unit
Mass of the ball	m	85.9×10^{-3}	kg
Gravitational acceleration	g	9.81	m/s ²
Resistance	r	2.1512	Ω
Inductance parameters	L_∞	54.9×10^{-3}	H
	a	15×10^{-3}	H
	b	50.4131	m ⁻¹

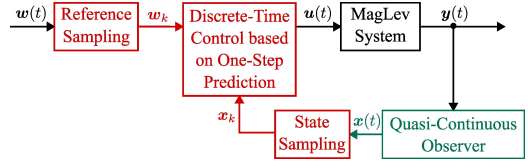


Fig. 2. Schematic block diagram of the experiment. Continuous-time components are drawn in black, quasi-continuous components in green, and discrete-time components in red.

found for the subsystem $[s, p]^T$. By the state transformation $z := i^2 - \phi(s, p)$, the system becomes

$$\underbrace{\begin{bmatrix} \dot{s} \\ \dot{p} \\ \dot{z} \end{bmatrix}}_{\hat{\dot{x}}} = \underbrace{\begin{bmatrix} \frac{p}{m} \\ mg + \frac{L'(s)}{2}(z + \phi) \\ f(s, p, z) \end{bmatrix}}_{f(\hat{x})} + \underbrace{\begin{bmatrix} 0 \\ 0 \\ g(s, p, z) \end{bmatrix}}_{\hat{G}(\hat{x})} u, \quad (37)$$

where

$$\begin{aligned} f(s, p, z) &= -\frac{2}{L(s)}(r + L'(s)\frac{p}{m})(z + \phi) - \dot{\phi}, \\ g(s, p, z) &= \frac{2\sqrt{z + \phi}}{L(s)}. \end{aligned} \quad (38)$$

For IDA-PBC, (37) with the control law $u = \hat{r}(\hat{x})$ (to be determined), is matched with the target dynamics $\hat{\dot{x}} = (\hat{J}_d - \hat{R}_d)\nabla\hat{H}_d(\hat{x})$, with the fictitious control law

$$\phi(s, p) = \frac{2}{L(s)}(-C(s - s^*) - k_1\frac{p}{m} - mg). \quad (39)$$

It can be verified that the matching conditions are satisfied with the interconnection and damping matrices

$$\hat{J}_d = \begin{bmatrix} 0 & 1 & 0 \\ -1 & 0 & \frac{L'(s)}{2} \\ 0 & -\frac{L'(s)}{2} & 0 \end{bmatrix}, \quad \hat{R}_d = \begin{bmatrix} 0 & 0 & 0 \\ 0 & k_1 & 0 \\ 0 & 0 & k_2 \end{bmatrix}, \quad (40)$$

and the closed-loop energy function

$$\hat{H}_d(\hat{x}) = \frac{p^2}{2m} + \frac{C}{2}(s - s^*)^2 + \frac{1}{2}z^2, \quad (41)$$

where $C, k_1, k_2 > 0$, and s^* is the desired position of the ball. The final control law is then obtained as

$$\hat{r}(s, p, z) = (\hat{G}^T \hat{G})^{-1} \hat{G}^T ((\hat{J}_d - \hat{R}_d)\nabla\hat{H}_d - \hat{f}). \quad (42)$$

Transforming (42) back to the original coordinates yields

$$r(s, p, i) = \hat{r}(s, p, i^2 - \phi(s, p)). \quad (43)$$

4.2 Experimental Results

We choose the control gains to be

$$C = m\lambda_s\lambda_p, \quad k_1 = -m(\lambda_s + \lambda_p), \quad k_2 = 80,$$

in which $\lambda_s, \lambda_p < 0$ are the desired eigenvalues of the subsystem $[s, p]^T$. Here we choose $\lambda_s = \lambda_p = -50$. Since the momentum p is not directly measurable, we use a quasi-continuous Luenberger observer operating at the base sampling time of 1 ms to mimic the state measurement as a proof of concept. The schematic block diagram for the conducted experiment is shown in Fig. 2. For the reference trajectory, we choose to switch between 2 setpoints s^* , smoothed by a low-pass filter with 0.05 s as the time constant.

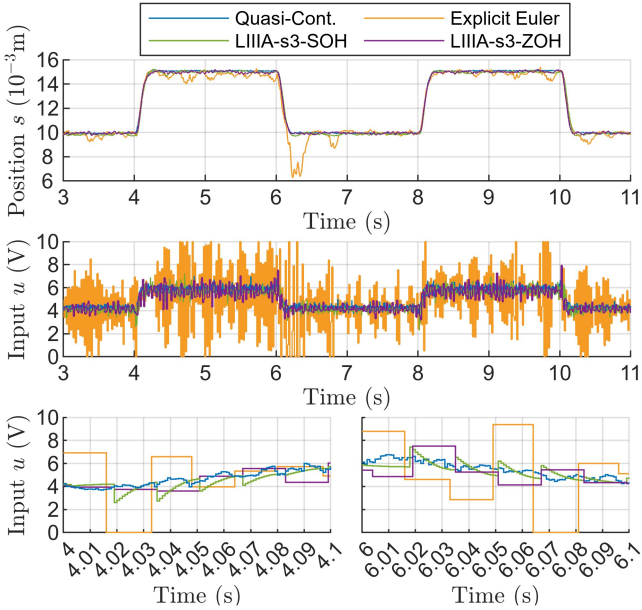


Fig. 3. Experimental results for the implementation of 3-stage Lobatto IIIA collocation at $h = 16$ ms.

Fig. 3 presents the experimental results of different control implementations. The quasi-continuous controller (“Quasi-Cont.”) is operating at the base sampling time (1ms) as a reference, while the other discrete-time controllers at $h = 16$ ms. We can see that at this relatively long sampling time, the traditional emulation control (“Explicit Euler”) struggles to remain stable. However, with the implementation of the 3-stage Lobatto IIIA method, both controllers using second-order-hold input (“LIIIA-s3-SOH”) and piecewise constant input (“LIIIA-s3-ZOH”) can follow the setpoint with very high accuracy.

Even though the 3-stage Lobatto IIIA collocation with SOH input provides very good result, we can see in the two plots at the bottom of Fig. 3, that the input signals have “serrated” shapes, which have a negative effect on the control performance. This effect is more dramatic with higher order approximations. As shown in Fig. 4, when implementing the 5-stage Lobatto IIIA collocation at $h = 11$ ms, the controller with fourth-order-hold input (“LIIIA-s5-FOH”) fails to provide as good accuracy as the one with piecewise constant input (“LIIIA-s5-ZOH”).

5. CONCLUSIONS AND OUTLOOK

In this contribution, we generalized Lobatto IIIA collocation and Hermite interpolation of arbitrary order towards the Hermite-Obreschkoff methods. We proved that when the nodes are the zeros of the shifted Legendre polynomial, the combination of Hermite-Obreschkoff formulas with pairs (n, m) , $n + m = s$ can be solved uniquely, and the solution yields Lobatto IIIA collocation and Hermite interpolation. In this sense, these two methods are equivalent.

Through experimental results with a new IDA-PBC control law for the MagLev system, we showed that the implementation of Hermite-Obreschkoff methods can indeed reduce the model mismatch and improve the performance of the controller. The results also justifies the conversion from higher-order-hold input to piecewise constant

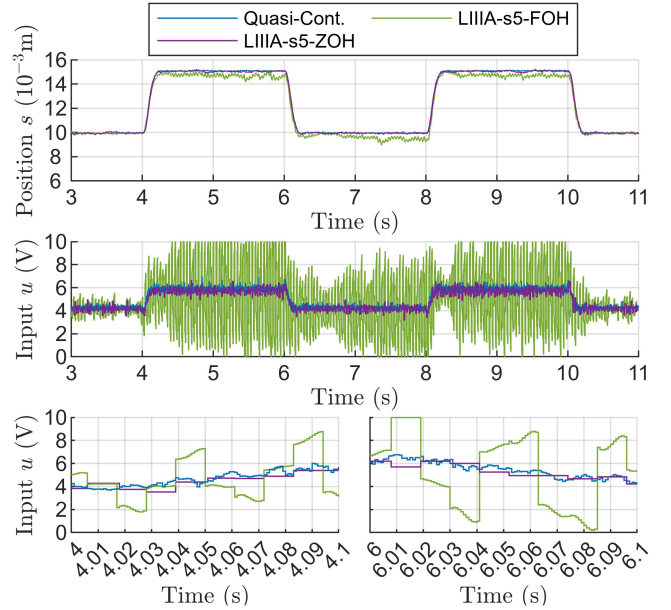


Fig. 4. Experimental results for the implementation of 5-stage Lobatto IIIA collocation at $h = 11$ ms.

input as it improves the performance of our higher-order discrete-time control.

As a further development, we currently investigate the relation between our higher-order discrete-time control and single-horizon model predictive control, and explore the possibility of consideration for constraints. It is also our interest to find out if the s -stage q -derivative collocation methods generalized by Kastlunger and Wanner (1972) could also be derived using the HO formula. In addition, regarding IDA-PBC design, we are currently working on exploiting the backstepping (strict-feedback) structure for the choice of the target system matrices.

REFERENCES

- Cesàro, E. (1890). *Sur la multiplication des séries*. Gauthier-Villars.
- Hairer, E., Lubich, C., and Wanner, G. (2006). *Geometric Numerical Integration: Structure-Preserving Algorithms for Ordinary Differential Equations*, volume 31 of *Springer Series in Computational Mathematics*. Springer-Verlag, Berlin, second edition.
- Jay, L.O. (1994). *Runge-Kutta type methods for index three differential-algebraic equations with applications to Hamiltonian systems*. Ph.D. thesis, University of Geneva, Switzerland.
- Kastlunger, K.H. and Wanner, G. (1972). Runge Kutta processes with multiple nodes. *Computing*, 9(1), 9–24.
- Khalil, H.K. (2002). *Nonlinear Systems*. Pearson Education. Prentice Hall.
- Kotyczka, P. (2023). Cubic Hermite interpolation and Lobatto collocation for nonlinear sampled-data control. *IFAC-PapersOnLine*, 56(2), 2883–2888. doi:10.1016/j.ifacol.2023.10.1406.
- Kotyczka, P., Martens, C.J., and Lefèvre, L. (2021). High order discrete-time control based on Gauss-Legendre collocation. *IFAC-PapersOnLine*, 54(19), 237–242. doi:10.1016/j.ifacol.2021.11.084.
- Kotyczka, P. and Thoma, T. (2021). Symplectic discrete-time energy-based control for nonlinear mechanical systems. *Automatica*, 133, 109842. doi:10.1016/j.automatica.2021.109842.
- Obreschkoff, N. (1940). Neue Quadraturformeln. *Abh. Preuss. Akad. Math. Nat. Kl.*, 4, 1–20.
- Ortega, R., van der Schaft, A., Maschke, B., and Escobar, G. (2002). Interconnection and damping assignment passivity-based control of port-controlled Hamiltonian systems. *Automatica*, 38(4), 585–596.